Lacunarity-Based Characterization of Hyperspectral Spatial Patterns

Anindita Das Bhattacharjee[1], Nibedan Banerjee[2], Debayudh Mitra[3], Tania Jamal[4], and Parthib Ghosh[5]

[1] IEM Centre of Excellence for InnovAI, Department of CSE, Institute of Engineering and Management, Kolkata, 700091, India, anindita.dasbhattacharjee@iem.edu.in,
[2] Institute of Engineering and Management, Kolkata, India banerjeenibedan@gmail.com,
[3] Institute of Engineering and Management, Kolkata, India debayudhmitra@gmail.com,
[4] Institute of Engineering and Management, Kolkata, India taniajamal2003@gmail.com,
[5] Institute of Engineering and Management, Kolkata, India parthibghosh786@gmail.com,

Abstract. This study explores image heterogeneity within the Salinas and Pavia University Datasets using lacunarity analysis. We identify the ”maximum information band” for each dataset based on standard deviation and analyze texture properties across different spatial scales within selected Regions of Interest (ROIs). Lacunarity patterns reveal transitions and saturation points, emphasizing the importance of scale selection for accurate texture characterization. Varying box sizes in Salinas ROIs affect lacunarity differently, with subtle variations in some and clearer patterns in others. In PaviaU, increasing box size initially increases lacunarity, then decreases, underscoring the need for optimal scale selection. The observed trends in lacunarity across ROIs highlight the complexity of texture structures, reflecting shifts in complexity and homogeneity at different scales. This study contributes to a deeper understanding of spatial heterogeneity and texture complexity in hyperspectral imagery, aiding in the identification of agricultural and urban features across various scales.

Keywords: Lacunarity, Statistical analysis, Hyperspectral data, Image heterogeneity, Remote Sensing

1 Introduction

Lacunarity analysis delineates spatial distribution and heterogeneity in images. In the Salinas dataset, reveals agricultural patterns; the Pavia University dataset unveils urban material distribution. Diverse box sizes are crucial for multi-scale exploration, ensuring efficient computation without compromising accuracy. This approach enhances understanding of spatial organization and complexity within

the datasets. When exploring lacunarity analysis within the Salinas and PaviaU datasets, selecting diverse box sizes is crucial. This diversity allows for thorough examination across multiple scales, capturing intricate details of both natural and artificial features. Different box sizes enable the detection of small-scale features like individual buildings and vegetation in PaviaU, and specific crop types in Salinas, while also revealing broader spatial structures. Balancing box size selection ensures computational efficiency without sacrificing accuracy. Analyzing lacunarity values across varied box sizes provides profound insights into the multi-scale nature of dataset features, enhancing understanding of spatial organization and complexity and improving subsequent analyses. This study aims to use lacunarity analysis to assess spatial distribution in Salinas and PaviaU datasets, revealing crop patterns and urban material distribution. Diverse box sizes are crucial for comprehensive pattern exploration, ensuring accurate analysis and understanding of multi-scale features.

2 Related Work

Hyperspectral imaging revolutionizes remote sensing [1], benefiting diverse industries [2]. Despite its advantages, processing hyperspectral data poses challenges [3], addressed by sophisticated statistical methods [4]. Lacunarity analysis assesses texture complexity and spatial heterogeneity numerically [5], providing insights into scene structures [6]. It complements traditional methods by capturing subtle details missed otherwise [7], revealing hidden environmental patterns [8]. Computational advancements facilitate lacunarity's widespread use in characterizing landscapes and monitoring ecosystem dynamics [9], aiding informed decision-making across domains [10]. The triangular prism method emerges as the most accurate for estimating fractal dimensions [12], capturing spatial structures efficiently [13]. The triangular prism method's sensitivity to sporadic speckles and lower dimensionality was noted [14]. Despite its accuracy in fractal dimension estimation, wavelet analysis may be more effective for characterizing spatial structures [15]. Although proficient in fractal dimension estimation, the triangular prism method struggles with the accurate classification of remote sensing images [15]. Lacunarity analysis extends beyond remote sensing, aiding landscape ecology [16]. A zonal lacunarity analysis tool evaluates grassland lacunarity across cities, highlighting spatial arrangement's importance in land use change assessment [16]. Pore lacunarity serves as an index for explaining soil variability due to land use changes, revealing shifts in pore distribution and soil properties [17]. This study employs lacunarity analysis to evaluate image heterogeneity, providing insights into spatial patterns and texture variation in hyperspectral imagery, benefiting diverse applications [18].We extensively explore lacunarity analysis in hyperspectral imagery, using advanced algorithms to assess spatial patterns and texture complexity across various scales. Focusing on specific Regions of Interest (ROIs) in the Salinas and PaviaU dataset, we aim to demonstrate lacunarity's utility as a quantitative metric for evaluating

texture variation and image heterogeneity. Our findings have implications for decision-making in land management, agriculture, remote sensing, and ecology.

3 Dataset

The Salinas dataset (Fig. 1), acquired by the Airborne Visible/Infrared Imaging Spectrometer (AVIRIS) over California's Salinas Valley, consists of 224 spectral bands with a spatial resolution of 512 by 217 pixels. Each pixel represents an agricultural area, offering detailed information on land cover and crop types across the 0.4 to 2.5-micrometer spectral range. It serves as a benchmark for hyperspectral image analysis, aiding research in classification, feature extraction, and land cover mapping. The Pavia University (Fig. 2) hyperspectral dataset, captured by the Reflective Optics System Imaging Spectrometer (ROSIS) over Pavia, Italy, comprises 115 spectral bands with a spatial extent of 610 by 340 pixels. Each pixel represents distinct urban or agricultural land cover, providing high-resolution information across the 0.43 to 0.86 micrometer spectral range. Python, with NumPy for numerical tasks, SciPy for MATLAB file loading and variance calculations, and Matplotlib for visualization, was used. Optional tools like OpenCV and scikit-learn were considered. A custom Gliding Box Lacunarity Distribution Algorithm aided lacunarity analysis. Data handling involved Salinas dataset manipulation, and Matplotlib facilitated visualization, with custom functions for gliding box lacunarity. The workflow included iterative steps from data loading to analysis.

(a) Salinas dataset: 224 bands, 512x217 pixels, 16 classes. Hyperspectral remote sensing for agricultural land use classification and vegetation analysis.

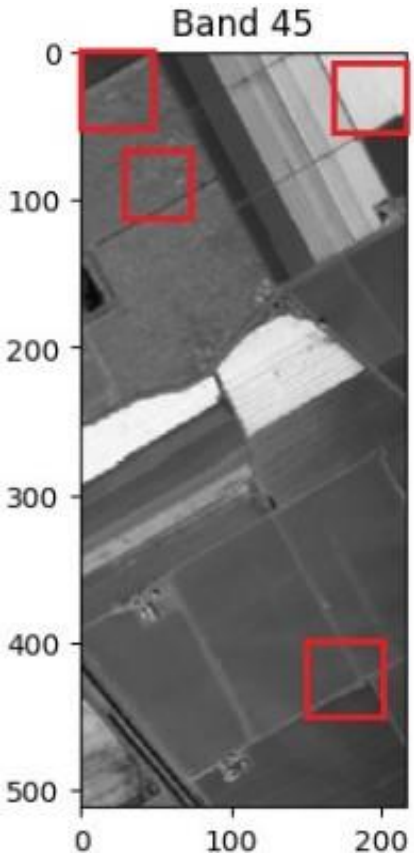

(b) Dividing the original image to find the optimal size for a gliding window/box.

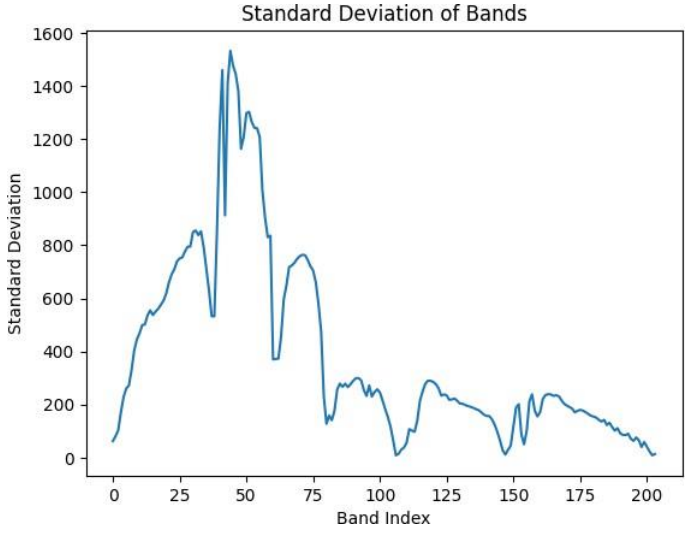

(c) Variation in Standard Deviation Across Hyperspectral Bands.

Fig. 1: a) The Salinas Dataset b)showcases the extraction of the most informative band(Band 45), and c)illustrates the change in standard deviation across all the bands of the Salinas dataset.

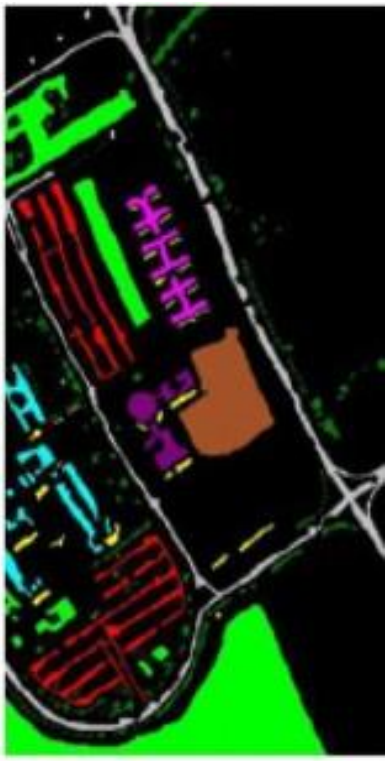

(a) PaviaU dataset: Hyperspectral imagery 610x340 pixels, 103 bands, used for classification in remote sensing and image processing.

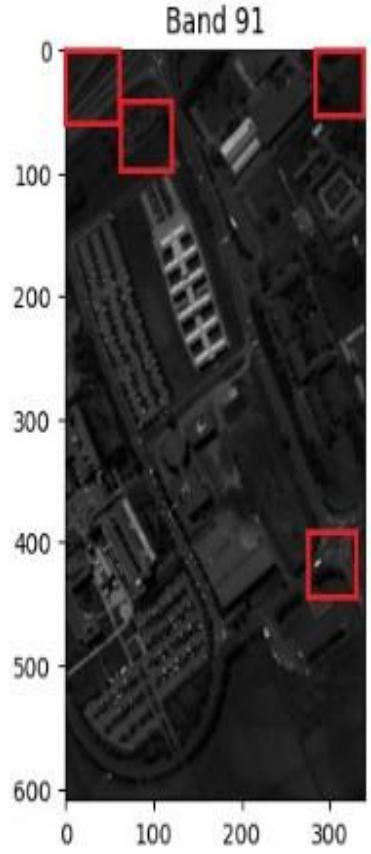

(b) Dividing the original image to identify an optimal gliding window/box.

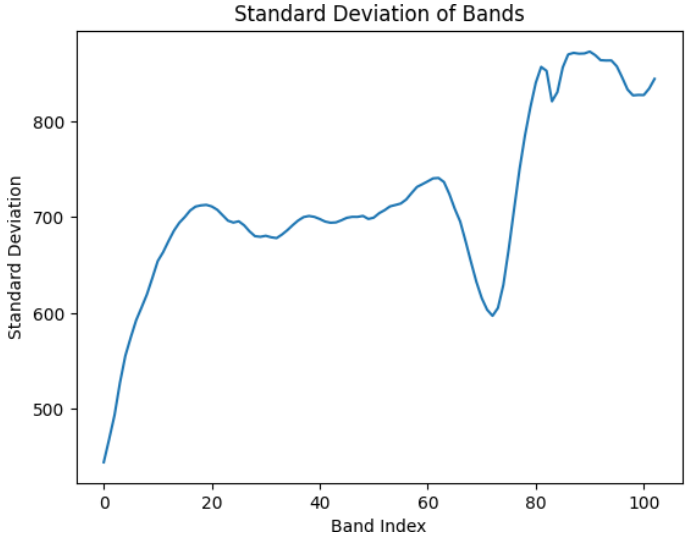

(c) Variation in standard deviation across all bands.

Fig. 2: a) The Pavia University Dataset, b)showcases the extraction of the most informative band(Band 91) and c)illustrates the change in standard deviation across all the bands of the PaviaU dataset.

This dataset is valuable for research in hyperspectral image analysis, enabling investigations into land cover classification, feature extraction, and environmental monitoring. This study explores both datasets to identify the band with the highest information content, crucial for capturing a broad range of scene elements. Hyperspectral data, treated as a 2D array, undergo statistical analysis to determine the ”maximum information band” based on the highest standard deviation. The chosen band is then subjected to gliding box approach lacunarity computation, enhancing discriminatory power in identifying textural variation within the hyperspectral data across spatial scales. This analytical approach contributes to a better understanding of hyperspectral datasets, advancing remote sensing applications.

4 Methodology

The sparsity of a dataset is quantified using the conventional concept of lacunarity, determined through a systematic gliding box approach outlined in Figure 3. In calculating gliding box lacunarity, sub-images within specified Regions of Interest (ROIs) are iteratively analyzed. The algorithm allocates points based on scale, adjusting states according to lacunarity and box count. Using a conditional image with fixed points states transition with scale changes. Matching set points to the box count at a scale allows the algorithm to progress, setting all allocated points to empty. Fewer set points result in allocated points marked as full, adhering to lacunarity constraints. Subsequently, pixels are subdivided into sub-pixels, inheriting states from the previous level. Equations 1, 2, and 3 illustrate the process of determining lacunarity for different box sizes.

$$\sigma^2 = \frac{\sum (x_i - \mu)^2}{N} \tag{1}$$

where,

σ^2 represents the variance.

x_i represents each unique label value within the sub-image.

μ represents the mean of the unique labels.

N represents the number of unique labels.

$$\Lambda = \frac{\sigma^2}{\mu} \tag{2}$$

where,

Λ represents the normalized variance, serving as the lacunarity value for the box.

σ^2 represents the variance calculated in step 1.

μ represents the mean of the unique labels.

$$\Lambda_{\text{mean}} = \frac{\sum_{i,j} \Lambda_{ij}}{M} \tag{3}$$

where,

Λ_{mean} represents the average lacunarity across the entire image for a given box size.

Λ_{ij} represents the lacunarity value at each pixel (i, j) in the lacunarity map.

M represents the total number of pixels in the lacunarity map.

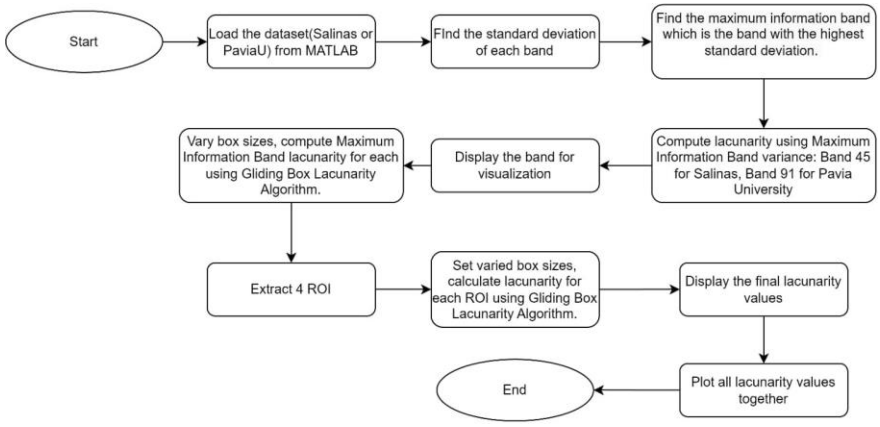

Fig. 3: The flowchart illustrates the procedure, starting with choosing informative bands from the Salinas and PaviaU datasets, and progressing to the application of the gliding box mechanism for Lacunarity analysis.

Fractals exhibit chaotic patterns, implying that the results are significantly influenced by the chosen box sizes in the computation process. Therefore, it becomes imperative to calibrate both the box and window sizes for optimal outcomes. Put differently, employing a small window size would restrict correlation detection to specific regions of the original image, while a larger window allows for the identification of more extensive patterns. The selection of an appropriate box size is also crucial. Different box sizes were employed to capture textural features at various spatial scales, contributing to the study's focus on four strategically positioned Regions of Interest (ROIs) within the dataset, each characterized by distinct spatial layouts. Band 45 is the maximum information band for salinas dataset while band 91 is the maximum information band for Pavia University dataset.In this study, we examined the spatial variability using the respective hyperspectral datasets(45 for salinas and 91 from Pavia University). This study delves into the intricate spatial dynamics using the respective hyperspectral datasets (band 45 for Salinas and band 91 for Pavia University). Employing an advanced gliding box lacunarity technique, we meticulously examined the textural attributes and spatial heterogeneity across diverse regions

of interest. The application of this methodology at various corners and with different box sizes facilitated a comprehensive multi-scale analysis, shedding light on the nuanced intricacies of texture modification.

5 Results

In the Salinas dataset shown in Figure 4 a), b), c), and d), ROI 4 initially exhibits elevated lacunarity, implying a composition characterized by diverse components contributing to its somewhat uneven and textured appearance.

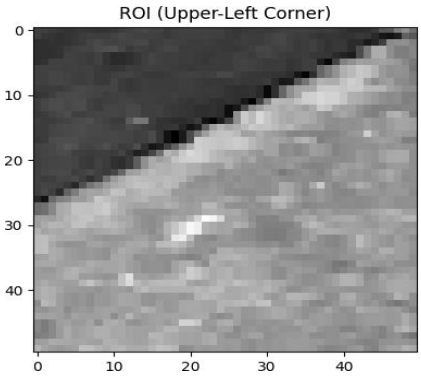

(a) ROI 1 (vineyard_untrained): Initially exhibits a declining pattern in smaller box sizes, with a subtle upward trend in larger boxes

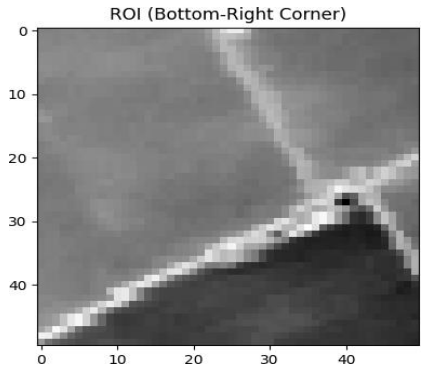

(b) ROI 2 (soil vineyard_develop): Demonstrates an ascending trend in values until reaching a threshold, followed by a declining trend.

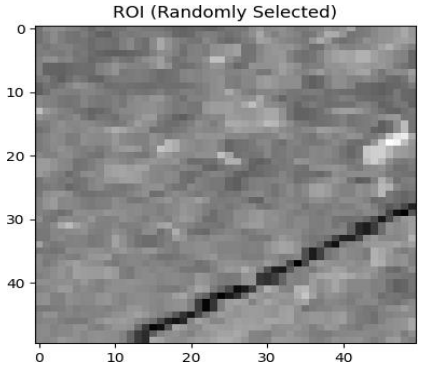

(c) ROI 3 (grapes untrained, vineyard_untrained): Shows an initial rise in lacunarity followed by a subsequent decline.

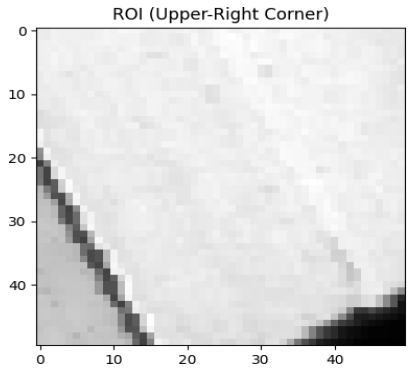

(d) ROI 4 (celery, stubble): Initially exhibits high lacunarity, followed by a sharp decrease in values as the box size increases.

Fig. 4: Lacunarity analysis of ROI 1, ROI 2, ROI 3 and ROI 4.

Table 1: Lacunarity values observed for various box sizes and regions of interest in the Salinas dataset.

Changes in Box Size	**Lacunarity Values**			
	ROI 1	ROI 2	ROI 3	ROI 4
2	4467.97	1288.58	2746.79	5869.42
4	4411.22	1704.33	4876.69	7532.84
8	675.23	2227.44	5267.64	4386.11
16	-2050.16	761.02	4211.83	-3716.82
32	58.91	-357.48	305.23	-99.77

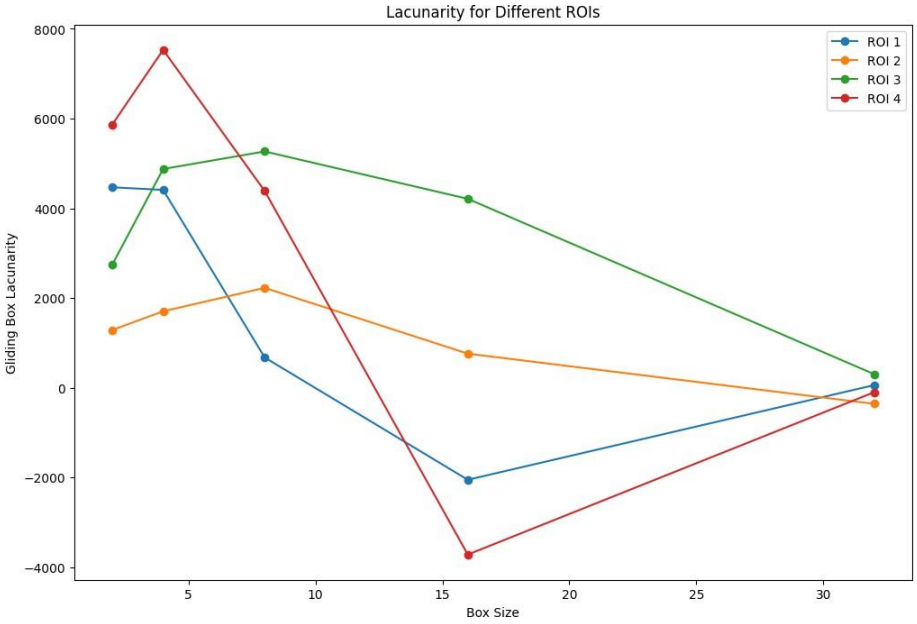

Fig. 5: Changes in gliding box lacunarity with varying box sizes.

However, with the enlargement of the box size, lacunarity sharply diminishes, signaling a transition toward a more homogeneous texture. ROI 2 demonstrates an inclining trend in lacunarity, indicative of a structured texture influenced by specific constituents. Intriguingly, as the box sizes increase, lacunarity in ROI 2 experiences a subtle decrease, implying a nuanced decrease in complexity or heterogeneity at broader spatial scales. On the other hand, ROI 3 portrays an initial upswing in lacunarity followed by a subsequent decline, suggesting a complex, multidimensional structure that becomes less pronounced as the box size

expands. Parallel to ROI 2, ROI 1 mirrors this behavior, exhibiting a trend akin to increasing lacunarity initially but deviating towards a slight decrease at larger box sizes. This indicates a less nuanced variation in texture complexity across spatial scales. In summary, the observed trends in lacunarity across different ROIs highlight the intricate nature of their textures. The changes in lacunarity with varying box sizes provide insights into the spatial distribution of features within each ROI, reflecting shifts in texture complexity and homogeneity at different scales.

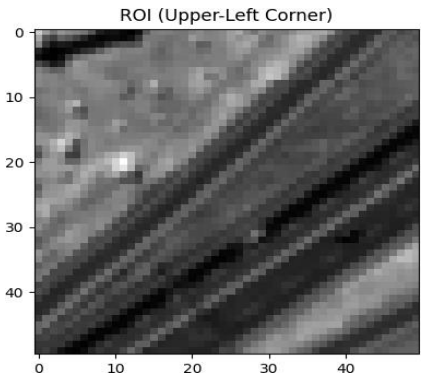

(a) ROI 1: Initially displays an upward trend in lacunarity, with a subsequent steady decrease beyond a specific threshold.

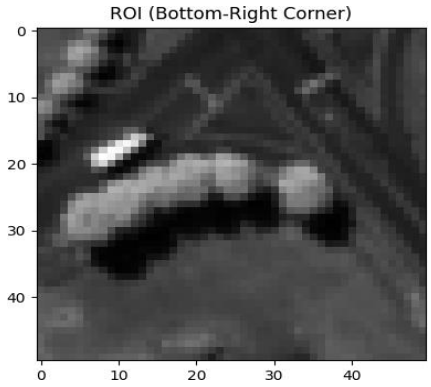

(b) ROI 2: Demonstrates an initial rise in lacunarity, followed by a steady decrease in values beyond a specific threshold.

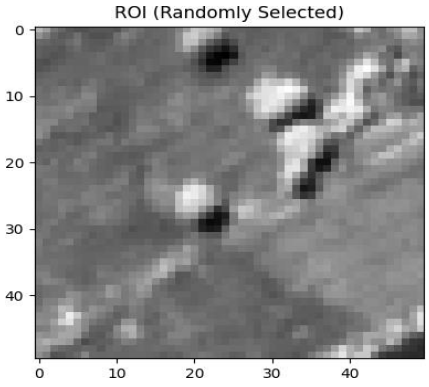

(c) ROI 3: Shows an initial rise in lacunarity, followed by a steady decrease in values beyond a specific threshold.

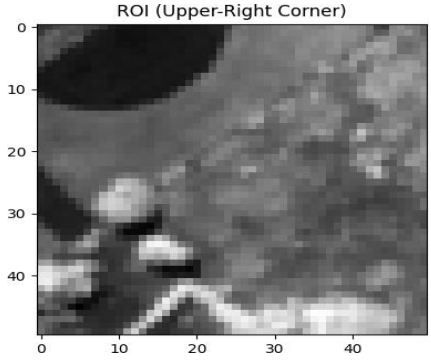

(d) ROI 4: Demonstrates an initial increase in lacunarity, followed by a steady decrease in values beyond a certain threshold.

Fig. 6: Lacunarity analysis of ROI 1, ROI 2, ROI 3 and ROI 4.

Table 2: Lacunarity values observed for various box sizes and regions of interest in PaviaU dataset.

Changes in Box Size	Lacunarity Values			
	ROI 1	ROI 2	ROI 3	ROI 4
2	19010.52	18587.92	16916.43	13694.23
4	27061.72	24665.64	24027.65	18935.35
8	24517.71	23426.36	23567.81	20483.07
16	15145.22	15460.85	15302.62	16452.79
32	5047.85	4492.98	4822.92	4813.53

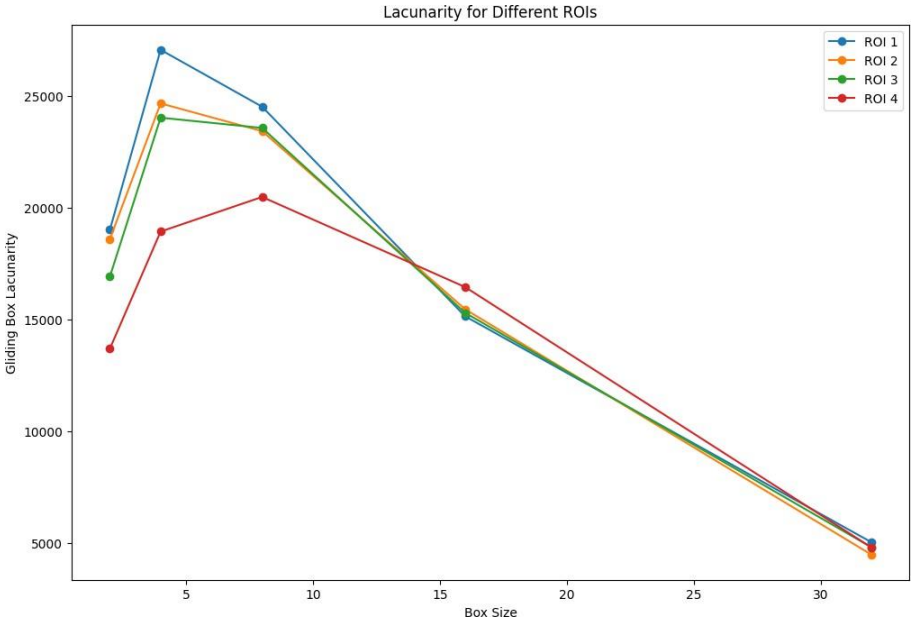

Fig. 7: Changes in gliding box lacunarity with varying box sizes.

In the PaviaU dataset shown in Figure 6 a), b), c), and d), an increase in box size initiates a simultaneous elevation in lacunarity for all Regions of Interest (ROIs), signifying a progressive shift towards more intricate and heterogeneous textures. This synchronized upward trend indicates that expanding the observation window captures additional details and intricacies within each ROI. However, beyond a certain threshold, lacunarity in all ROIs begins a steady decline. This descent implies a saturation point, where the inclusion of further spatial information yields diminishing returns in terms of texture complexity.

The decreasing trend after this critical point suggests that the addition of more context from larger observation windows results in a simplification of perceived texture, potentially due to the averaging out of finer details or the emergence of more uniform patterns at broader spatial scales. This observation emphasizes the significance of discerning the optimal scale or window size for effectively characterizing texture complexity in hyperspectral imagery across various regions of interest. Understanding this optimal scale is crucial for accurately interpreting and representing the intricate spatial patterns inherent in hyperspectral data, ensuring a nuanced analysis of texture complexity tailored to specific ROIs within the PaviaU dataset.

6 Conclusion

The choice of lacunarity calculation method depends on data characteristics and research goals. Variance suits simple patterns, while closest neighbor analysis is effective for gap details. For complex designs, consider box-counting or multifractal analysis. For large datasets or real-time applications, prioritize computationally efficient techniques like variance or Morisita's index. Each method has its pros and cons, guided by analysis goals, data properties, interpretability, and computational demands. Lacunarity analysis finds applications in ecological studies, urban planning, precision agriculture, and remote sensing, offering insights for land use efficiency and biodiversity assessment. It aids in understanding spatial complexity in diverse landscapes, promoting sustainable practices. Gliding box lacunarity variations are depicted in Figures 5 and 7, and corresponding values in Tables 1 and 2 for Salinas and PaviaU datasets.

References

1. Plaza, A., et al. (2009). Recent advances in techniques for hyperspectral image processing. Remote Sensing of Environment, 113(1), S110-S122. doi:10.1016/j.rse.2007.12.013
2. Smith, A.M.S., Milton, E.J., and Pelizzari, A. (2019). Hyperspectral Remote Sensing of Vegetation. CRC Press.
3. Boardman, J.W. (1997). Hyperspectral remote sensing of vegetation and agricultural crops. Photogrammetric Engineering & Remote Sensing, 63(7), 727-734.
4. Atzberger, C. (2013). Advances in remote sensing of agriculture: Context description, existing operational monitoring systems and major information needs. Remote Sensing, 5(2), 949-981. doi:10.3390/rs5020949
5. Mandelbrot, B.B. (1982). The fractal geometry of nature. WH Freeman and Company.
6. Plotnick, R.E., et al. (1996). Lacunarity analysis: A general technique for the analysis of spatial patterns. Physical Review E, 53(5), 5461-5468. doi:10.1103/PhysRevE.53.5461
7. Mehmood, T., et al. (2017). Hyperspectral image classification using deep learning architectures. Remote Sensing, 9(4), 357. doi:10.3390/rs9040357

8. Ghosh, S., and Sengupta, D. (2020). Recent trends in lacunarity analysis in remote sensing applications: A review. ISPRS Journal of Photogrammetry and Remote Sensing, 164, 125-144. doi:10.1016/j.isprsjprs.2020.04.003
9. Chakraborty, A., et al. (2018). Lacunarity analysis for land cover classification using multitemporal ALOS-2 PALSAR-2 polarimetric data. IEEE Journal of Selected Topics in Applied Earth Observations and Remote Sensing, 11(7), 2434-2445. doi:10.1109/JSTARS.2018.2828163
10. Olson, M.A., and Gupta, A. (2017). Exploring the utility of lacunarity analysis in detecting landscape patterns associated with invasive plant species. Applied Geography, 80, 63-73. doi:10.1016/j.apgeog.2016.10.010
11. Liu, J., and Zhang, K. (2019). A review on hyperspectral remote sensing techniques for land cover classification and mapping. IEEE Journal of Selected Topics in Applied Earth Observations and Remote Sensing, 12(5), 1693-1711. doi: 10.1109/JSTARS.2019.2905903
12. Lam, N. S. N., Qiu, H. L., Quattrochi, D. A., Emerson, C. W., & Arnold, J. E. (2001). An Evaluation of Fractal Surface Measurement Methods for Characterizing Landscape Complexity from Remote-Sensing Imagery.
13. Hua-Jiang, D. U., Xian-Wen, D. I. A. O., & Wen-Xi, F. A. N. (2011). Fractal Dimensions Being An Index of Bands Selection for Hyper-spectral Remote Sensing Data. Remote Sensing Technology and Application, 19(1), 5-9.
14. Qiu, H. L., Lam, N. S. N., Quattrochi, D. A., & Gamon, J. A. (1999). Fractal characterization of hyperspectral imagery. Photogrammetric Engineering and Remote Sensing, 65(1), 63-71.
15. Zhao, W. (2001). Multiscale analysis for characterization of remotely sensed images. Louisiana State University and Agricultural & Mechanical College.
16. Dong, P., Sadeghinaeenifard, F., Xia, J., & Tan, S. (2019). Zonal lacunarity anal- ysis: a new spatial analysis tool for geographic information systems. Landscape Ecology, 34, 2245-2249. doi:10.1007/s10980-019-00884-0
17. Santos, C. R. D., Antonino, A. C. D., Heck, R. J., Lucena, L. R. R. D., Oliveira, A. C. H. D., Silva, A. S. A. D., ... Menezes, R. S. C. (2020). 3D soil void space lacunarity as an index of degradation after land use change. Acta Scientiarum. Agronomy, 42, e42491.